ORIGINAL ARTICLE

The Three Horizons Problem: How Long Can Particle-Horizon Acceleration Last?

OpenAI's ChatGPT[1] | A. J. H. Thys[2]

[1]Main contributor; AI system
[2]Independent Researcher, Belgium

Correspondence
A. J. H. Thys
Email: bth247@gmail.com
ORCID: 0009-0001-4606-2296
Earlier preprint DOI:
10.5281/zenodo.24427303
Manuscript revised 25 November 2026

A growing coefficient in an inverse-square particle-horizon density can make a dust universe accelerate. How many e-folds of uninterrupted acceleration are compatible with a finite ceiling? For flat general relativity with conserved dust we derive a sharp bound from the initial matter fraction, the particle radius in Hubble lengths and the coefficient ceiling. Coasting attains the bound, and strictly accelerating solutions approach it arbitrarily closely. For a big-bang past of nonpositive total pressure, we identify the coefficient threshold for acceleration consistent with the null energy condition. An explicit solution with continuous pressure crosses into acceleration and back while satisfying that condition throughout. In every expanding solution of this class that reaches arbitrarily large scale factor, the expansion speed tends to zero and the remaining conformal time is infinite. At the apparent horizon, two assignments of conserved matter reproduce the same expansion and give residual densities of opposite sign near redshift one. At the event horizon a radius ceiling depends on the full future expansion. The particle-horizon duration bound can be evaluated at the beginning of an accelerating interval.

1 | INTRODUCTION

In a universe with a decelerating matter component, can a density tied to the distance light has travelled since the big bang sustain a second era of acceleration? With a fixed inverse-square coefficient, Li (2004) found that the particle-horizon prescription gives a component pressure too high to drive acceleration in the dominant-component limit. The corresponding one-fluid particle- and event-horizon power laws have also been worked out by Cruz & Lepe (2020). A variable coefficient reopens the question. Radicella & Pavón (2010) found the coefficient required to reproduce a prescribed vacuum density. Here the future expansion is unknown and only a finite upper limit on the coefficient is specified.

Write the candidate energy density as

$$\varepsilon_X(t) = \frac{BF(t)}{R_X(t)^2}, \qquad B > 0, \qquad 0 \le F(t) \le 1. \tag{1}$$

The constant B has units of energy per length, F is the fraction of the coefficient ceiling in use, and R_X is a proper horizon radius. The particle radius accumulates past null propagation. The apparent radius in a flat universe is the instantaneous Hubble length. The event radius depends on all subsequent null propagation (Davis & Lineweaver, 2004; Harrison, 1991; Margalef-Bentabol, Margalef-Bentabol, & Cepa, 2013; Re Fiorentin & Re Fiorentin, 2023; Rindler, 1956). These three choices have distinct consequences even at the level of the homogeneous expansion.

For the particle horizon the Friedmann equation gives two results. First, on every allowed unbounded expansion the speed $\dot{a}$ tends to zero. Second, a measured or stipulated starting state and a specified B set a maximum duration of uninterrupted nondeceleration. Section 2.1 derives that maximum and identifies the expansion that attains it. We construct two finite episodes. The first changes the sign of the total acceleration through a brief rise in density. The second respects the null energy condition in each component, with a unique transition back to deceleration. Transient acceleration also occurs in scalar-field cosmology (Carvalho, Alcaniz, Lima, & Silva, 2006). The restriction derived here uses the particle radius and the bounded coefficient explicitly.

The apparent- and event-horizon comparisons in Sections 3 and 4 ask which parts of this argument survive a change of radius. We use comoving proper time t, a dimensionless scale factor a, and $H = \dot{a}/a > 0$. Each example specifies its own reference epoch. Energy density and pressure have the same units.

2 | A BOUNDED PARTICLE-HORIZON SOURCE CANNOT SUSTAIN ACCELERATION

A constant amplitude multiplying R_p^{-2} gives a particle-horizon component with pressure ratio $w_p > -1/3$ in the component-dominated calculation of Li (2004). Allowing the amplitude to grow changes its instantaneous pressure and reopens the question of acceleration. The following result requires only an upper bound on the amplitude.

Proposition 1 (particle-horizon bound). Consider a spatially flat, simply connected FLRW universe in general relativity with constant G. Its sources are positive separately conserved dust of energy density $\varepsilon_{m0}a^{-3}$ and a component of energy density $BF(t)/R_p(t)^2$, with constant $B > 0$ and $0 \le F(t) \le 1$. Normalize the dimensionless scale factor a to unity today and use comoving proper time t. Suppose the solution expands to arbitrarily large a and its comoving particle radius is finite and strictly positive at some regular epoch t_*. Then the future conformal-time interval is infinite and $\dot{a} \to 0$. In particular, there is no finite future event horizon, and no future interval extending to infinity on which $\ddot{a} \ge 0$ throughout.

Proof. The proper particle radius $R_p = a\chi_p$ includes the comoving distance $\chi_p = \int_{t_i}^{t} c\,dt'/a(t')$ already traversable by light since the past boundary t_i. Substitution in the Friedmann equation gives

$$\dot{a}^2 = \frac{A}{a} + \frac{KF}{\chi_p^2}, \qquad \dot{\chi}_p = \frac{c}{a}, \qquad A = \frac{8\pi G\varepsilon_{m0}}{3c^2}, \quad K = \frac{8\pi GB}{3c^2}. \tag{2}$$

Both terms in $\dot{a}^2$ have units of inverse time squared. After t_*, each denominator increases, even if F varies rapidly. With $a_* = a(t_*)$, $\chi_* = \chi_p(t_*)$ and $V_* = (A/a_* + K/\chi_*^2)^{1/2}$, it follows that $\dot{a} \le V_*$. Reaching arbitrarily large a requires infinite proper time. The linear upper bound $a(t) \le a_* + V_*(t - t_*)$ now gives

$$\chi_p(t) - \chi_* \ge \frac{c}{V_*} \ln\left[1 + \frac{V_*(t - t_*)}{a_*}\right]. \tag{3}$$

The right-hand side diverges, so light can cover arbitrarily large comoving distances in the future. Returning to Eq. (2), both A/a and KF/χ_p^2 tend to zero. Thus $\dot{a} \to 0$. If $\ddot{a} \ge 0$ for every $t \ge T$, then $\dot{a}(t) \ge \dot{a}(T) > 0$ there, contradicting this limit. ∎

The same proof includes separately conserved radiation, which adds a term proportional to a^{-2} to Eq. (2). A positive cosmological constant would instead contribute a growing term proportional to a^2. The result permits episodes of acceleration and places no restriction on the sign of $\dot{F}$.

2.1 | How long can one accelerating episode last?

Fix a starting epoch t_s in the dust model of Proposition 1. Write $v_s = \dot{a}(t_s) > 0$, $a_s = a(t_s)$, $\chi_s = \chi_p(t_s) > 0$ and $H_s = v_s/a_s$. Three dimensionless quantities specify the bound.

$$m = \frac{A}{a_s v_s^2} = \Omega_m(t_s), \qquad \beta = \frac{v_s\chi_s}{c} = \frac{H_s R_p(t_s)}{c}, \qquad \alpha = \frac{K}{c^2}. \tag{4}$$

Here $0 < m \le 1$ is the starting dust fraction, β measures the starting particle radius in Hubble lengths, and α fixes the physical amplitude ceiling.

Proposition 2 (duration at fixed initial state). If the expansion speed stays nondecreasing from t_s to t, the number of e-folds $N = \ln[a(t)/a_s]$ and the elapsed proper time obey

$$N \le N_{\max}, \qquad H_s(t - t_s) \le e^{N_{\max}} - 1, \qquad (1 - me^{-N_{\max}})(\beta + N_{\max})^2 = \alpha. \tag{5}$$

These bounds are sharp for the forward problem when only the starting state and amplitude ceiling are fixed.

Proof. Set $v = \dot{a}$, $Y = v\chi_p/c$ and $\Omega_m = A/(av^2)$. Equation (2) gives $\alpha F = (1 - \Omega_m)Y^2$. Since $d\chi_p/dN = c/v$, nondecreasing speed gives, at the endpoint,

$$Y(N) = \frac{v(N)\chi_s}{c} + \int_0^N \frac{v(N)}{v(n)}\,dn \ge \beta + N, \qquad \Omega_m(N) = me^{-N}\frac{v_s^2}{v(N)^2} \le me^{-N}. \tag{6}$$

Thus $(1-me^{-N})(\beta+N)^2 \le \alpha F(N) \le \alpha$. The left side increases strictly from $\alpha F(t_s)$ to infinity, which proves existence and uniqueness of $N_{\max}$, including $N_{\max} = 0$ at initial saturation. Integrating $dt = da/v$ with $v \ge v_s$ gives the time bound.

Coasting at $v = v_s$ attains both comparisons on the forward interval. The required fraction is $F = (1 - me^{-N})(\beta + N)^2/\alpha$. For any endpoint strictly below $N_{\max}$, the speeds $v = v_s e^{\delta N}$ with sufficiently small $\delta > 0$ give strict acceleration throughout that interval. Their required fractions converge uniformly to the coasting fraction, so they remain within the ceiling. Their elapsed times likewise approach the coasting time. Thus even with strict acceleration the bounds are suprema. A prescribed past derivative or a smooth join at saturation can further restrict an individual trajectory. ∎

The coasting extremum requires total pressure $-\varepsilon_{\mathrm{tot}}/3$, all carried by the horizon component. Thus $\varepsilon_X + P_X = (2/3 - \Omega_m)\varepsilon_{\mathrm{tot}}$, and the effective component obeys the null energy condition throughout if $m \le 2/3$, since $\Omega_m = me^{-N}$.

A weaker consequence independent of the starting dust fraction and radius is $N^2(1 - e^{-N}) < \alpha$ for every positive-length episode. For $\alpha = 1$ this already excludes 1.19702 e-folds of uninterrupted nondeceleration. At the onset of acceleration in Fig. 1 , $m = 0.998431$, $\beta = 2.001570$, and $H_s T = 0.664101$ in the units of Section 2.2. Equation (5) gives $N_{\max} = 0.223951$ and $(t - t_s)/T \le 0.377969$. The actual episode lasts 0.060119 e-folds or $0.089504T$. The bound uses the state at onset and the amplitude ceiling. It requires no choice of the subsequent opening law.

2.2 | Acceleration during a rapid rise in amplitude

A rapidly changing amplitude can reverse the sign of the acceleration for a finite time. Differentiating Eq. (2) on the expanding branch gives the exact condition

$$\ddot{a} > 0 \quad \Longleftrightarrow \quad \dot{F} > \frac{A\dot{a}\,\chi_p^2}{Ka^2} + \frac{2Fc}{a\chi_p}. \tag{7}$$

The two terms are the effects of dust dilution and the growth of the comoving particle radius. With a constant or decreasing F, the dust term alone ensures deceleration whenever the dust density is positive.

For a regular example with a particle radius fixed by its physical past, choose the reference epoch $T > 0$, write $\theta = t/T$, $x = \chi_p/(cT)$, and let a prime denote differentiation with respect to θ. Set $AT^2 = 4/9$, $K/c^2 = 1$. For $0 < \theta \le 1$ take the pure dust solution $a = \theta^{2/3}$, $x = 3\theta^{1/3}$, $F = 0$. Increase F from zero to unity over $1 < \theta < 1.1$ as $F = 3u^2 - 2u^3$, $u = 10(\theta - 1)$, and keep $F = 1$ thereafter. This fraction and its first derivative are continuous at both joins.

At the midpoint $\theta = 1.05$, $F = 1/2$ and $F' = 15$. Over the first half of the transition $a \ge 1$, $3 \le x \le 3.05$ and $a' \le \sqrt{5}/3$ by Eq. (2). The right side of Eq. (7), multiplied by T, is at most $(4/9)(\sqrt{5}/3)(3.05)^2 + 1/3 < 3.42$. Thus $a'' > 0$ on an open interval about the midpoint. After $\theta = 1.1$ the model again decelerates. The upper bounds on a' and $x' = 1/a$ preclude finite-time divergence, and $a' \ge 2/(3\sqrt{a})$ gives $a^{3/2}(\theta) \ge \theta$ for $\theta \ge 1$. This same solution therefore expands to arbitrarily large a and obeys the proposition.

Figure 1 locates both sign changes and follows the same trajectory past saturation. The construction prescribes a homogeneous source. As ε_X first rises from zero, separate conservation requires $\varepsilon_X + P_X = -\dot{\varepsilon}_X/(3H) < 0$ during part of the transition. At $\theta = 1.05$, the solution gives $T^2\dot{H} = 0.44453 > 0$. The total stress tensor therefore violates the null energy condition at the midpoint. Section 2.3 constructs a distinct trajectory for which both components satisfy it.

2.3 | A finite accelerating interval consistent with the null energy condition

Can the particle-horizon source accelerate the expansion while its own density decreases or stays constant? Let $\varepsilon_\Lambda > 0$ denote its early density and choose $a = 1$ at equality with dust, so $\varepsilon_m = \varepsilon_\Lambda a^{-3}$. Set $H_\Lambda^2 = 8\pi G\varepsilon_\Lambda/(3c^2)$, $L = 2c/H_\Lambda$, $B = 2\varepsilon_\Lambda L^2$ and $r = R_p/L$. This fixes $8\pi GB/(3c^4) = 8$. A continuously differentiable amplitude that increases monotonically to its ceiling is

$$F(r) = \begin{cases} r^2/2, & 0 < r \le 1, \\ 1 - (2-r)^2/2, & 1 < r < 2, \\ 1, & r \ge 2. \end{cases} \tag{8}$$

The dimensionless density $e = \varepsilon_X/\varepsilon_\Lambda = 2F/r^2$ equals $1, -1 + 4/r - 2/r^2$, and $2/r^2$ on the three branches. Its derivative is zero on the first branch and strictly negative on both later branches. With $h = H/H_\Lambda = \sqrt{a^{-3} + e}$, the identity $\dot{R}_p = HR_p + c$ and separate conservation give

$$\frac{\varepsilon_X + P_X}{\varepsilon_\Lambda} = -\frac{1}{3}\left(r + \frac{1}{2h}\right)\frac{de}{dr} \ge 0. \tag{9}$$

The pressure is continuous at both joins. The dust density is positive, so $\dot{H} < 0$ throughout the expansion.

On the constant-density branch the null integral from the big bang gives $r(a) = a\int_0^{\sqrt{a}}(1 + y^6)^{-1/2}\,dy$. In particular $r(1) < 1$, so this branch includes equality. Acceleration starts at $a = 2^{-1/3}$, when $\varepsilon_m = 2\varepsilon_\Lambda$, and the deceleration parameter $q = -\ddot{a}/(aH^2)$ reaches $-1/4$ at equality. For $a \ge 1$, $H_\Lambda a^{-3/2} \le H \le \sqrt{2}H_\Lambda$ ensures expansion to arbitrarily large a in infinite proper time. The increasing radius reaches $r = 2$ in finite time since $\dot{R}_p \ge c$. Thereafter the constant amplitude gives $P_X/\varepsilon_X = -1/3 + 2c/(3HR_p) > -1/3$, and the expansion decelerates permanently.

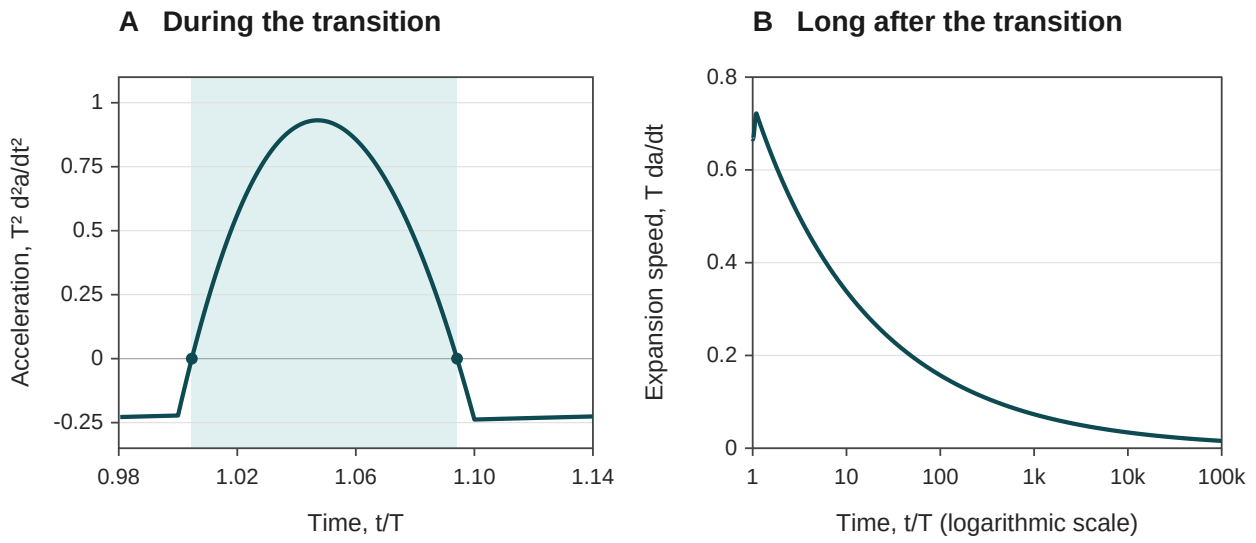


FIGURE 1 Transient acceleration from a bounded particle-horizon amplitude. The past is the flat dust solution with $a(T) = 1$ and $\chi_p(T) = 3cT$. For $T < t < 1.1T$, the fraction rises from zero to one as $F = 3u^2 - 2u^3$, $u = (t - T)/(0.1T)$, and remains at one thereafter. The parameters are $AT^2 = 4/9$ and $K/c^2 = 1$. In panel A the shaded interval $1.00465 < t/T < 1.09415$ has $\ddot{a} > 0$. Panel B follows the same solution over five decades in time. The eventual limit $\dot{a} \to 0$ follows from the proposition.

There is exactly one exit from acceleration. On the intervening branch, write $m = a^{-3}$. Substitution of Eq. (9) in the acceleration equation gives

$$\frac{2r\ddot{a}}{aH_\Lambda^2} = 4 - 2r - mr - \frac{2(r-1)}{hr^2}, \qquad 1 < r < 2. \tag{10}$$

Here $(r-1)/r^2$ and $1/h$ both increase. Since $d\ln r/d\ln a = 1 + 1/(2hr) > 1$, one has $d(mr)/dr > -2m$. The derivative of the right-hand side with respect to r is therefore less than $-2 + 2m < 0$. Its endpoint signs are opposite. Numerically, acceleration ends at $a = 1.42610$, before saturation at $a = 1.75699$ (Fig. 2). At onset $m = 2/3$ in the notation of Proposition 2 and $\beta = 2.37587$. The interval lasts 0.58599 e-folds, within its sharp initial-state limit of 0.92301 e-folds.

The duration depends on the physical ceiling. At fixed ε_Λ, choosing L larger than the particle radius at any specified finite endpoint of the dust-plus-constant-density solution preserves that solution up to the endpoint. Increasing $B = 2\varepsilon_\Lambda L^2$ accordingly permits arbitrarily many accelerating e-folds across this family.

This construction specifies a continuous homogeneous stress history. Immediately above $r = 1$, $d\varepsilon_X/dr$ approaches zero from below while dP_X/dr approaches a positive finite limit, so $dP_X/d\varepsilon_X \to -\infty$. In a single adiabatic barotropic perfect fluid, the squared sound speed would therefore be $c^2\, dP_X/d\varepsilon_X < 0$ immediately after the join. Component null energy condition satisfaction does not establish perturbative stability. A physical completion must specify the additional stress dynamics and test its perturbations on this background.

2.4 | A sharp amplitude threshold for a nonpositive-pressure past

Consider an expanding flat dust-plus-X solution from a Big Bang at $a = 0$. Suppose the total pressure has been nonpositive throughout the past of an epoch a, and the component obeys $\varepsilon_X + P_X \geq 0$ at that epoch. Write $\alpha = 8\pi GB/(3c^4)$, $Y = HR_p/c$, and $\Omega_X = 8\pi G\varepsilon_X/(3c^2H^2) = \alpha F/Y^2$. Conservation gives $d\ln H/d\ln a = -3(1 + w_{\rm tot})/2 \geq -3/2$, where $w_{\rm tot} = P_{\rm tot}/\varepsilon_{\rm tot}$. Thus $H(a') \leq H(a)(a/a')^{3/2}$ for $0 < a' < a$, and

$$Y = aH(a)\int_0^a \frac{da'}{a'^2H(a')} \geq 2, \qquad \Omega_X \leq \frac{\alpha}{4}. \tag{11}$$

Acceleration requires $\varepsilon_{\rm tot} + 3P_X < 0$. Since $P_X \geq -\varepsilon_X$, this implies $\Omega_X > 1/3$. Consequently $\alpha > 4/3$ is necessary. In particular, the critical coefficient $\alpha = 1$ excludes acceleration under these pressure conditions. The bound uses nonpositive total pressure over the entire preceding expansion; it does not directly apply to a radiation-dominated past.

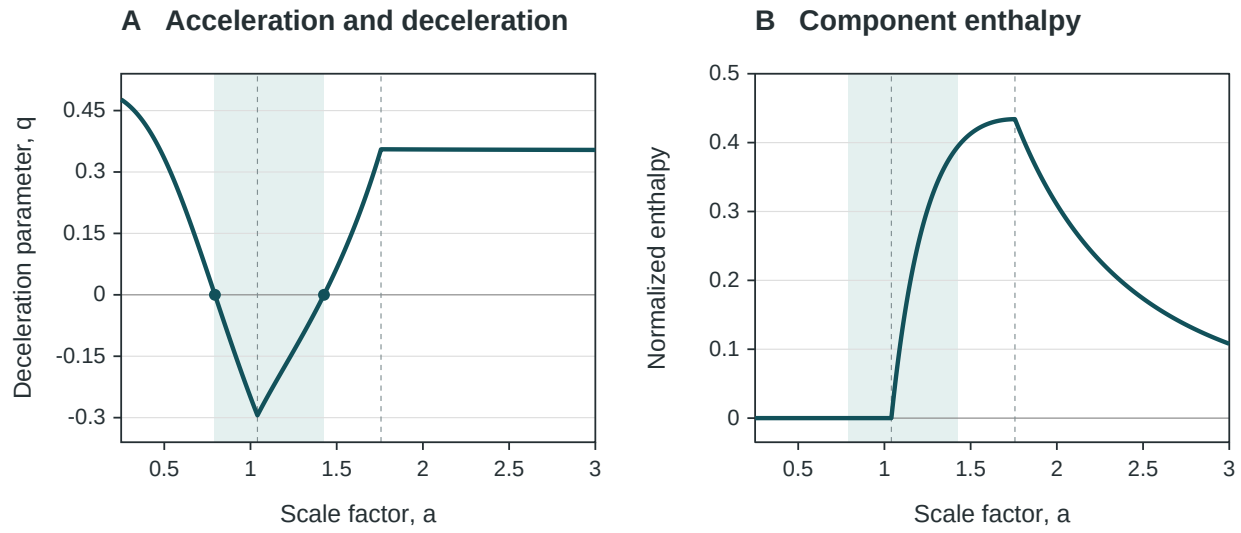


FIGURE 2 A bounded particle-horizon source with nonnegative enthalpy. The shaded interval in both panels is the epoch of acceleration, $0.79370 < a < 1.42610$. Panel A shows the total deceleration parameter. Panel B shows the source density plus pressure in units of ε_Λ. The vertical guides mark $R_p = L$, where the density begins to fall, and $R_p = 2L$, where the amplitude saturates.

The threshold is sharp for continuous densities with finite pressure jumps. For any $\alpha > 4/3$, choose $1/3 < f < \min(1, \alpha/4)$. Begin with $a \propto t^{2/3}$, $R_p = 3ct$, and two pressureless components with $\Omega_X = f$, $\Omega_m = 1 - f$ and $F = 4f/\alpha < 1$. At a regular epoch t_s, hold ε_X fixed at its value there, giving $P_X = -\varepsilon_X$. The dust density decreases, so Ω_X increases from $f > 1/3$ and the expansion accelerates. The total pressure was zero before t_s and is negative throughout this interval. Meanwhile $F = (4f/\alpha)[R_p/R_p(t_s)]^2$ reaches unity in finite proper time because $\dot{R}_p = HR_p + c \geq c$.

Thereafter set $F = 1$. Conservation gives $P_X/\varepsilon_X = -1/3 + 2/(3Y) > -1/3$, hence the expansion decelerates for the entire remaining future. Positive dust gives $\dot{a} \geq \sqrt{A/a}$, while deceleration bounds $\dot{a}$ from above, so the solution reaches arbitrarily large a in infinite time. The density and expansion speed match at both transitions, and each phase obeys the component null energy condition.

2.5 | Required amplitudes and the distinction from material area

Suppose a universe with the same dust content is required to follow $a(t) = a_*(t/t_*)^p$ for $t \geq t_* > 0$, with $p > 1$. Its comoving particle radius approaches the finite length $\chi_\infty = \chi_* + ct_*/[a_*(p-1)]$. Solving the Friedmann equation for the required fraction gives

$$F_{\rm req}(t) = \frac{\chi_p^2}{K}\left(\dot{a}^2 - \frac{A}{a}\right) \sim \frac{\chi_\infty^2}{K}\left(\frac{pa_*}{t_*}\right)^2\left(\frac{t}{t_*}\right)^{2p-2}. \quad (12)$$

Even for p arbitrarily close to one from above, the required fraction eventually exceeds unity. The divergence quantifies the failure of this prescription for a specified expansion history. At the coasting limit $p = 1$ the power-law asymptote in Eq. (12) ceases to apply. Here $\dot{a} = a_*/t_*$ is constant and $\chi_p = \chi_* + (ct_*/a_*)\ln(t/t_*)$, so the required fraction still diverges, as $(c^2/K)\ln^2(t/t_*)$.

A conserved component whose material transverse area grows as a^2 provides a useful comparison. Let its full energy density be $\varepsilon_s = \Sigma a^{-2}$, with constant $\Sigma > 0$, so that $P_s = -\varepsilon_s/3$. Expressing the same density through the true particle radius requires

$$BF_{\rm req} = \varepsilon_s R_p^2 = \Sigma\chi_p^2. \quad (13)$$

With positive conserved dust and this component as the only sources in flat general relativity, $\dot{a}^2 = A/a + 8\pi G\Sigma/(3c^2)$. The expansion approaches coasting and its accumulated comoving particle radius diverges. Thus $BF_{\rm req}$ grows without bound. This material-area example lies outside the finite particle-horizon coefficient class of Proposition 1; an area proportional to a^2 is not the area of the particle horizon.

Published particle-horizon models illustrate the scope of this bound. The density used by Abdollahi Zadeh, Sheykhi, Moradpour, & Bamba (2018) in their Eq. (20) scales as $R_p^{2\delta-4}$. Its effective inverse-square coefficient, $\varepsilon_X R_p^2$, scales as $R_p^{2\delta-2}$. When $\delta > 1$ this coefficient grows without bound along an unbounded expansion with an existing particle horizon. The case $\delta = 2$ gives a constant density and makes the required quadratic growth of the coefficient explicit. Another proposed law sets the density proportional to $\ddot{R}_p/R_p$ (Fazlollahi, 2023). Applying the proposition to that law would require a non-negative, bounded effective coefficient proportional to $R_p\ddot{R}_p$, together with the stated matter content.

2.6 | A necessary condition at the other two horizons

Suppose a dust model using the apparent or event radius has an infinite future with $H = \dot{a}/a \to H_\infty > 0$. The apparent radius $R_A = c/H$ tends to c/H_∞. The event radius $R_e = c\int_0^\infty a(t)/a(t+u)\,du$ has the same limit. Indeed, once $|H - H_\infty| < \delta < H_\infty$ throughout the future tail, integrating the exponential bounds on $a(t)/a(t+u)$ confines R_e between $c/(H_\infty+\delta)$ and $c/(H_\infty-\delta)$. The dust density vanishes in this limit. For either prescription the Friedmann equation therefore requires

$$\lim_{t\to\infty} \alpha F(t) = 1, \qquad \alpha = \frac{8\pi G B}{3c^4}. \tag{14}$$

Hence $\alpha \geq 1$, with $\alpha = 1$ if the full reserve becomes accessible asymptotically. This necessary condition leaves the existence of such a solution to the evolution law for F and, in the event case, the future boundary condition.

3 | THE APPARENT HORIZON AND TWO ASSIGNMENTS OF CONSERVED MATTER

In spatially flat general relativity, consider the illustrative expansion $H/H_0 = 0.70 + 0.30a^{-3/2}$, with $a = 1$ today. This is the $A = 0.70$ member of the Model 1 family of Durán & Parisi (2012). Their noninteracting decomposition assigns $\Omega_{m0} = (1-A)^2 = 0.09$. The value $A = 0.70$ is chosen here for illustration; their reported best fit is $A = 0.588 \pm 0.004$. Table 1 compares the illustrative 9% assignment with 30% conserved dust at the same $H(a)$. At $a = 1/2$, both assignments give a Hubble rate of $1.5485\,H_0$ and the same total pressure. Subtracting dust leaves a positive component density of 1.6779 present critical densities in the first case and a negative remainder of -0.0021 in the second. The zero in the second decomposition occurs at $z = 0.998734$. We derive the boundary for an arbitrary dust assignment and lookback interval.

3.1 | A constant rate at the apparent horizon

Consider a spatially flat universe containing only conserved dust and a component X with radius $R_A = c/H$. Let $B > 0$ be the maximum inverse-square amplitude, in units of energy per length. A constant rate $\Gamma > 0$ per unit of the remaining inaccessible reserve gives

$$\begin{aligned} \varepsilon_X &= \frac{BF}{R_A^2}, \qquad \dot{F} = \Gamma(1-F), \\ \alpha &= \frac{8\pi G B}{3c^4} > 0. \end{aligned} \tag{15}$$

At proper time t, $1 - F = (1-F_0)\exp[-\Gamma(t-t_0)]$, where $F_0 = F(t_0)$. The fraction stays in $[0, 1)$ to the future for $0 \leq F_0 < 1$. Its past domain depends on the assigned dust density.

The density fraction in X is αF. With $H_0 = H(t_0)$ and conserved dust of density $\varepsilon_{m0}a^{-3} > 0$, the Friedmann equation reads

$$\begin{aligned} (1-\alpha F)E^2 &= \Omega_{m0}a^{-3}, \\ \Omega_{m0} &\equiv \frac{\varepsilon_{m0}}{\varepsilon_{\mathrm{crit},0}} = 1 - \alpha F_0, \\ \varepsilon_{\mathrm{crit},0} &= \frac{3c^2H_0^2}{8\pi G}. \end{aligned} \tag{16}$$

The expansion rate and deceleration parameter follow by differentiation,

$$\begin{aligned} \frac{2\dot{H}}{H} &= -3H + \frac{\alpha\Gamma(1-F)}{1-\alpha F}, \\ q &\equiv -\frac{a\ddot{a}}{\dot{a}^2} = \frac{1}{2} - \frac{\alpha\Gamma(1-F)}{2H(1-\alpha F)}. \end{aligned} \tag{17}$$

For $0 < \alpha < 1$, $1-\alpha F \to 1-\alpha$. Dust-like expansion resumes at late times, with $a \propto t^{2/3}$ and $q \to 1/2$, even if an earlier phase accelerated. For $\alpha > 1$, the expanding positive-dust branch reaches $F = 1/\alpha$ at

$$t_s - t_0 = \frac{1}{\Gamma}\ln\left(\frac{1-F_0}{1-1/\alpha}\right). \tag{18}$$

As $t \to t_s$, the factor $1 - \alpha F$ vanishes linearly. Hence

$$\frac{d(a^{3/2})}{dt} = \frac{3H_0}{2}\sqrt{\frac{\Omega_{m0}}{1-\alpha F(t)}} \propto (t_s - t)^{-1/2}.$$

This divergence is integrable. The scale factor remains finite as H diverges. These two futures leave $\alpha = 1$ as the candidate for asymptotically constant positive H when $F \to 1$, in accord with Eq. (14).

TABLE 1 Two conserved-dust assignments for the illustrative expansion $E(a) = 0.70 + 0.30a^{-3/2}$. These parameters are not the observational best fit reported by Durán & Parisi (2012). The common columns give $E = H/H_0$ and $\widehat{P} = P_{\rm tot}/\varepsilon_{\rm crit,0}$. Dust has zero pressure. For each assignment, $\widehat{\varepsilon}_X = \varepsilon_X/\varepsilon_{\rm crit,0}$, $F = \widehat{\varepsilon}_X/E^2$, and $w_X = \widehat{P}/\widehat{\varepsilon}_X$ on the positive-density branch.

	Common expansion		$\Omega_{m0} = 0.09$			$\Omega_{m0} = 0.30$		
a	E	$\widehat{P}$	F	$\widehat{\varepsilon}_X$	w_X	F	$\widehat{\varepsilon}_X$	w_X
1	1.0000	−0.7000	0.91000	0.9100	−0.7692	0.70000	0.7000	−1.0000
2/3	1.2511	−0.8758	0.80595	1.2616	−0.6942	0.35318	0.5528	−1.5842
0.5	1.5485	−1.0840	0.69974	1.6779	−0.6460	−0.00086	−0.0021	—
0.4	1.8859	−1.3201	0.60459	2.1502	−0.6139	−0.31803	−1.1311	—

3.2 | Critical normalization and homogeneous pressure

At $\alpha = 1$ the fraction of total density in X equals the accessible fraction F. For positive dust, the ratio $(1-F)/(1-\alpha F)$ cancels from Eq. (17). With $s = \Gamma/(3H_0)$ one obtains

$$\frac{dH}{d\ln a} = \frac{\Gamma - 3H}{2}, \qquad E(a) = s + (1-s)a^{-3/2}, \qquad q(a) = \frac{1}{2} - \frac{3s}{2E(a)}. \tag{19}$$

The future limit is $H_\infty = \Gamma/3$. The Hubble rate falls toward that limit for $0 < s < 1$, is constant for $s = 1$, and rises for $s > 1$. We consider $0 < s < 1$, which gives a dust-like expansion at small a. Since the dust pressure vanishes, $P_X = P_{\rm tot}$. Combining $P_{\rm tot}/\varepsilon_{\rm tot} = -1 - 2\dot{H}/(3H^2)$ with the dust subtraction gives

$$\frac{\varepsilon_X}{\varepsilon_{\rm crit,0}} = E^2 - \Omega_{m0}a^{-3} = FE^2, \qquad \frac{P_X}{\varepsilon_{\rm crit,0}} = -sE, \tag{20}$$

$$w_X = -\frac{s}{EF} \quad (F > 0), \qquad w_{\rm tot} = -\frac{s}{E}. \tag{21}$$

These expressions give the homogeneous stress required by the expansion. The conservation of the total source and of dust implies separate conservation of the remainder. A physical stress law, including its perturbations, requires further input.

Two published models also realize this total pressure. The expression $P_{\rm tot} = -\Gamma c^2 H/(8\pi G)$ equals the bulk-viscous pressure $-3\zeta H$ at constant $\zeta = \Gamma c^2/(24\pi G)$ (Avelino & Nucamendi, 2009). It also equals the adiabatic creation pressure $-\Gamma\varepsilon_{\rm tot}/(3H)$ for dust with a constant creation rate per particle (Lima, Silva, & Santos, 2008). Here the assigned dust is separately conserved. On this branch any independently specified $H(a)$ would require

$$\Gamma_{\rm inferred}(a) = 3H + \frac{2\dot{H}}{H} = H(1-2q). \tag{22}$$

Constancy of this quantity tests the assumed rate. Positivity of the residual gives a separate constraint on the dust abundance.

3.3 | Which part of the history has nonnegative density?

For any positive $E(a)$ on the critical branch, $F = 1 - \Omega_{m0}a^{-3}/E^2$. The residual-density positivity criterion of L'Huillier, Shafieloo, & Kim (2018), with equality admitted at zero density, is

$$\Omega_{m0} \le \inf_{a\in I}\{a^3E(a)^2\}. \tag{23}$$

In the constant-rate solution the entire fraction history is explicit,

$$F(a) = 1 - \frac{\Omega_{m0}}{[1 - s + sa^{3/2}]^2}, \qquad F_0 = 1 - \Omega_{m0}, \qquad 0 < s < 1. \tag{24}$$

It rises monotonically with a and stays below unity. Thus the earliest epoch decides admissibility on $[a_{\rm min}, 1]$, where $0 < a_{\rm min} < 1$. The necessary and sufficient condition is

$$1 - s + sa_{\rm min}^{3/2} \ge \sqrt{\Omega_{m0}}. \tag{25}$$

In the limit $a_{\rm min} \to 0$, the same condition can be expressed using the rate, current acceleration, or current component pressure.

$$s \le 1 - \sqrt{\Omega_{m0}}, \qquad q_0 \ge -1 + \frac{3}{2}\sqrt{\Omega_{m0}}, \qquad w_{X0} \ge -\frac{1}{1 + \sqrt{\Omega_{m0}}}. \tag{26}$$

For $0 < \Omega_{m0} < 1$, a vacuum-like residual pressure today would require $s = 1 - \Omega_{m0}$, strictly above $1 - \sqrt{\Omega_{m0}}$. Hence a component matching vacuum pressure today reaches zero density at a finite past epoch. More generally, whenever the all-past bound fails, the first zero in a backward extrapolation occurs at

$$a_{\rm on} = \left(\frac{\sqrt{\Omega_{m0}} - (1-s)}{s}\right)^{2/3}. \tag{27}$$

The expansion itself is regular at this boundary. The density changes sign there while P_X remains finite and negative, so w_X is undefined at the crossing.

The independent dust assignment selects the side of the boundary. Writing $u = a^{-3/2}$, one finds

$$\frac{\varepsilon_X}{\varepsilon_{\rm crit,0}} = s^2 + 2s(1-s)u + \left[(1-s)^2 - \Omega_{m0}\right]u^2. \tag{28}$$

The coefficient of u^2 determines the early-time sign. A positive coefficient leaves a dust-like remainder with $w_X \to 0$. A zero coefficient removes the leading dust term, leaving $\varepsilon_X \propto a^{-3/2}$, $F \to 0$, and $w_X \to -1/2$. At equality, $s = A$ and $\Omega_{m0} = (1-A)^2$ reproduce both densities and the amplitude $\tilde{c}^2 = F$ in Eqs. (18), (21)–(23) of Durán & Parisi (2012). Further, $D(a) = 1 - s + sa^{3/2}$ obeys $\dot{D}/D = 3sH_0/2$, so $1 - F = \Omega_{m0}/D^2$ yields the constant $\dot{F}/(1-F) = 3sH_0$ for this member of their model family.

For the illustrative $s = 0.70$, both assignments in Table 1 share $q_0 = -0.55$. The 9% assignment saturates the all-past bound and has $w_{X0} = -0.76923$. The 30% assignment gives $w_{X0} = -1$ and $a_{\rm on} = 0.500317$. At that abundance, Eq. (26) would require $q_0 \geq -0.17842$ for positivity throughout the past.

In the second decomposition the fraction rises through the present while the density reaches a maximum. The component enthalpy is

$$\frac{\varepsilon_X + P_X}{\varepsilon_{\rm crit,0}} = a^{-3}\left[s(1-s)a^{3/2} + (1-s)^2 - \Omega_{m0}\right]. \tag{29}$$

It is negative between $a_{\rm on}$ and today, vanishes at $a = 1$, and becomes positive thereafter. Since $\dot{\varepsilon}_X = -3H(\varepsilon_X + P_X)$, the density first increases and subsequently falls toward $s^2\varepsilon_{\rm crit,0}$. The total enthalpy $\varepsilon_{\rm crit,0}E(E-s)$ remains positive throughout. A finite interval with $w_X < -1$ can therefore occur while the total Hubble rate decreases.

4 | WHICH RADIUS DOES AN EXPANSION HISTORY SPECIFY?

Two universes can agree on their complete expansion history up to today and assign different event horizons to the same observer today. The particle horizon depends on the preceding expansion, the apparent horizon on the instantaneous expansion, and the event horizon on the future continuation. We use proper radii on constant cosmic-time slices of a spatially flat FLRW spacetime with simply connected spatial sections. The dimensionless scale factor is normalized by $a(t_0) = 1$, $H = \dot{a}/a > 0$, and χ is a comoving radial coordinate of dimension length. A radial null ray obeys $d\chi/dt = \pm c/a$, so proper and areal radius are both $R = a\chi$ (Davis & Lineweaver, 2004; Harrison, 1991; Rindler, 1956).

For cosmic-time endpoints t_i, t_f the three radii are

$$\begin{aligned} R_p(t) &= a(t)\int_{t_i}^{t}\frac{c\,dt'}{a(t')}, \\ R_e(t) &= a(t)\int_{t}^{t_f}\frac{c\,dt'}{a(t')}, \\ R_A(t) &= \frac{c}{H(t)}. \end{aligned} \tag{30}$$

Each integral horizon exists as a finite radius where its integral converges. Where both exist, $(R_p + R_e)/a$ is constant. The flat apparent radius is the sphere at which an ingoing null wavefront has stationary area, since $\dot{R} = HR - c$ on the ray (Cai & Kim, 2005). This local condition permits subsequent crossing of the sphere.

At differentiable epochs set $q = -a\ddot{a}/\dot{a}^2$ and $\gamma_X = d\ln R_X/d\ln a$. Differentiating Eq. (30) with endpoints fixed gives

$$\begin{aligned} \dot{R}_p &= HR_p + c, & \gamma_p &= 1 + \frac{c}{HR_p}, \\ \dot{R}_A &= c(1+q), & \gamma_A &= 1 + q, \\ \dot{R}_e &= HR_e - c, & \gamma_e &= 1 - \frac{c}{HR_e}. \end{aligned} \tag{31}$$

The integral-radius equations admit a homogeneous term proportional to a. The endpoint conditions $R_p/a \to 0$ as $t \to t_i$ and $R_e/a \to 0$ as $t \to t_f$ fix the respective constants. A measured radius history would give $H = (\dot{R}_p - c)/R_p$ or $H = (\dot{R}_e + c)/R_e$ wherever the radius is positive. Recovering H this way establishes a local identity. Identifying the proposed radius as the causal boundary also requires its endpoint condition.

4.1 | One emission event and two possible futures

Let $a(t) = a_*(t/t_*)^{2/3}$ from the initial singularity through t_*. On that slice $H_* = 2/(3t_*)$, $R_p = 3ct_*$ and $R_A = 3ct_*/2$. Emit an ingoing photon at proper distance $2c/H_*$. If dust expansion continues indefinitely, the photon arrives at $t = 8t_*$, since

$$a_*\int_{t_*}^{t}\frac{c\,dt'}{a(t')} = 3ct_*\left[(t/t_*)^{1/3} - 1\right] = 2c/H_*. \tag{32}$$

If instead $a = a_*\exp[H_*(t-t_*)]$ thereafter, the same emission lies outside the event radius c/H_*. Both continuations match a and $\dot{a}$ at the join. A smooth transition with the same asymptotic tails preserves the distinction between finite and infinite remaining conformal time.

Even the sign of future acceleration is insufficient to decide convergence. For $a = (t/T)\ln(t/T)$ on $t > eT$, with $T > 0$, one has $\ddot{a} = 1/(Tt) > 0$ and $\int dt/a$ diverges as $T \ln\ln(t/T)$. An exponent $1+\delta$, $\delta > 0$, on the logarithm makes the integral converge. For an exact power law $a \propto t^{\nu}$, $\nu > 0$, the particle integral at zero converges for $\nu < 1$, giving $R_p = ct/(1-\nu)$. The event integral at infinity converges for $\nu > 1$, giving $R_e = ct/(\nu-1)$. At $\nu = 1$ both endpoint integrals diverge logarithmically. The accelerating power law also illustrates a separate issue. A convergent future integral can give a proper event radius that grows without bound.

4.2 | An event radius bounded by future apparent radii

For a flat expansion with $H > 0$, $a \to \infty$ and a convergent future conformal integral, the event radius is an average of future apparent radii. Substitution of $u = a/a'$ gives

$$R_e(a) = ac\int_a^{\infty} \frac{da'}{a'^2 H(a')} = \int_0^1 R_A(a/u)\,du, \qquad R_A(a) = \frac{c}{H(a)}. \tag{33}$$

Let $M_X(I) = \sup_{a\in I} R_X(a)$ and let $R_{\mathrm{cap}} > 0$ be a proposed common radius ceiling. For $I = [a_0, \infty)$ every sampled argument lies in I. Bounding the integrand by $M_A(I)$ gives

$$M_e(I) \le M_A(I), \qquad M_A(I) \le R_{\mathrm{cap}} \quad \Rightarrow \quad M_e(I) \le R_{\mathrm{cap}}. \tag{34}$$

Thus any common ceiling respected by the apparent radius over the full future is also respected by the event radius. On a finite interval the average extends past the interval's upper limit. The converse can fail even on the full future. For the smooth example $R_A(a) = L(1 + 0.20/a)$ at $a \ge 1$, Eq. (33) gives $R_e(a) = L(1 + 0.10/a)$. The ceiling $1.15L$ admits the event radius throughout, while the apparent radius exceeds it until $a = 4/3$.

Monotonicity gives additional pointwise information. For a nondecreasing R_A, each averaged radius is at least $R_A(a)$, hence $R_e(a) \ge R_A(a)$. The event radius also increases or stays constant, since each integrand does so. If $R_A \to L < \infty$, the average is trapped between $R_A(a)$ and L, and both radii approach L. If $R_A \to \infty$, R_e is unbounded as well. For a nonincreasing R_A the pointwise inequality reverses. Without monotonicity Eq. (34) still holds, but a shared asymptotic length could be exceeded earlier by either history.

5 | PHYSICAL INTERPRETATION

5.1 | A common expansion and different sources

The three horizon histories are calculable once the complete expansion and its endpoints are given. Consequently, two decompositions of the stress tensor that agree on the entire expansion give identical values of each respective radius. The 9% and 30% dust assignments in Section 3 agree on the formal $H(a)$ yet disagree on the past domain of the residual. In this comparison the matter abundance must be specified independently of the residual whose sign is being tested. Appendix D gives a second, everywhere positive example of the same ambiguity and shows how separate conservation fixes the pressure along a chosen density history (Durán & Parisi, 2012; Kunz, 2009).

There is a related absolute-scale ambiguity. Multiplying G by a constant $\lambda > 0$ while dividing every density and pressure by λ preserves both homogeneous Einstein equations and the continuity equations. Hence it preserves all three radii at matched endpoints. An absolute density measurement can break this rescaling. To distinguish models with the same background after fixing G, one would need further physical information, for example a prediction for how their constituents cluster. The homogeneous pressure on a given trajectory leaves its pressure perturbations and anisotropic stress undetermined.

5.2 | When a radius ceiling becomes a physical test

In the prescribed-expansion comparisons the simplest exclusion needs only two independent inputs. Suppose the fraction in use today has lower bound f_-, and a candidate radius at a later epoch exceeds r_- times its present value. For constant target density and radius exponent $D > 0$, Eq. (B11) requires a fraction at least $f_- r_-^D$. A product above unity excludes the model over that interval. Statistical bounds on the two inputs must have joint coverage if they share the same reconstructed $H(a)$. For an event horizon the geometric input also inherits the uncertainty of the future continuation.

The upper limit on the amplitude has operational meaning only if the physical model assigns it independently. A microscopic interpretation would have to identify the reserve, determine which part is accessible, and relate that part to a gravitating energy density with the requisite units. For $D = 2$, a numerator with units of energy requires a further length to produce an energy per volume. An opening process would also have to account for the pressure inferred from the continuity equation. Without those inputs the bounds constrain families of proposed source terms.

6 | CONCLUSIONS

Once the starting dust fraction m, particle radius in Hubble lengths β, and ceiling $\alpha = 8\pi GB/(3c^4)$ are specified, the upper limit on the duration of uninterrupted acceleration is fixed. For N e-folds of uninterrupted nondeceleration the necessary inequality is

$$(1 - me^{-N})(\beta + N)^2 \leq \alpha.$$

Its limiting trajectory coasts. At fixed starting state and ceiling, strictly accelerating solutions can approach the same limiting interval. In the first example the bound permits 0.22395 e-folds and the actual episode uses 0.06012. This is a test that uses initial data and an independently specified coefficient ceiling. Varying the ceiling changes the physical model.

The temporary acceleration can occur with nonincreasing density in each component. In the regular example the horizon density starts at a finite constant, the total expansion accelerates, and the growth of the particle radius eventually ends acceleration as the inverse-square coefficient approaches saturation. With a big-bang past of nonpositive total pressure, null-energy-condition preserving acceleration requires $\alpha > 4/3$ (Section 2.4). Every unbounded solution of the bounded particle-horizon model still has $\dot{a} \to 0$ and infinite remaining conformal time. This result constrains a homogeneous stress history. A prediction for clustering or a microscopic implementation requires further dynamics.

For the apparent radius, fixing the expansion fixes the total density in flat general relativity. The positivity of a residual component then depends on the independently assigned matter abundance. For the event radius, the decisive input is the continuation of the expansion into the future. These distinctions explain why the bound on the duration of particle-horizon acceleration does not transfer to the other radii by substitution.

DATA AND CODE AVAILABILITY

All numerical examples are theoretical. The accompanying supplementary package contains the vector figures, their generation scripts, tabulated histories and checks of the sharp duration bound, both particle-horizon trajectories, the apparent-horizon density tests and the geometric calibrations. It also includes an independently implemented numerical verifier and its recorded outputs. The methods and cross-checks are described in Appendix F.

CONTRIBUTOR ROLES

OpenAI's ChatGPT is the main contributor to the mathematical development, calculations, numerical verification, code, figure generation, and manuscript drafting and revision. A. J. H. Thys supplied the original research ideas and questions, guided the conceptual direction, and serves as the human collaborator and corresponding author. The numerical methods and cross-checks are described in Appendix F.

APPENDIX A: PAST-DOMAIN TESTS FOR THE APPARENT-HORIZON RECONSTRUCTION

A.1 The lookback interval and the matter bound

At the illustrative value $s = 0.70$, Eq. (25) gives maximum present dust fractions of 0.090, 0.228 and 0.445 for intervals beginning at $a \to 0$, 0.40 and 0.65, respectively (Fig. A1).

Imposing $w_{X0} = -1$ fixes $s = 1 - \Omega_{m0}$ and leaves a single parameter in the crossing epoch,

$$a_{\rm on} = \left(\frac{\sqrt{\Omega_{m0}}}{1 + \sqrt{\Omega_{m0}}} \right)^{2/3}, \qquad 0 < \Omega_{m0} < 1. \tag{A1}$$

As Ω_{m0} increases from zero toward unity, $a_{\rm on}$ increases from zero toward $2^{-2/3}$.

A.2 Effect of separately conserved radiation

How sensitive is the finite past boundary to radiation? Retain the critical normalization and constant rate, and define $M = \Omega_{m0} + \Omega_{r0}$, $0 < M < 1$, with $P_r = \varepsilon_r/3$. Write

$$\begin{aligned} E_B(a) &= \sqrt{\frac{\Omega_{m0} a^{-3} + \Omega_{r0} a^{-4}}{M}}, \\ Y &= \exp\left[\tfrac{1}{2} \Gamma (t - t_0) \right]. \end{aligned} \tag{A2}$$

The opening law gives $1 - F = M/Y^2$. The expanding Friedmann branch gives $E = E_B Y$, hence $dY/da = 3s/(2aE_B)$. With $Y(1) = 1$, this integrates to

$$\begin{aligned} Y(a) &= 1 - \frac{3s}{2} \big[J(1) - J(a) \big], \\ J(a) &= \int_0^a \frac{dx}{x E_B(x)} = \frac{2a^2}{3} \frac{v(a) + 2u}{[v(a) + u]^2}, \end{aligned} \tag{A3}$$

where $u = \sqrt{\Omega_{r0}/M}$, $v(a) = \sqrt{u^2 + (1 - u^2)a}$, and $J(0) = 0$. Since Y increases, positivity throughout $[a_{\rm min}, 1]$ is equivalent to $Y(a_{\rm min}) \geq \sqrt{M}$. The criterion for all $a > 0$ up to the present is

$$s \leq (1 - \sqrt{M}) \frac{(1 + u)^2}{1 + 2u}. \tag{A4}$$

Equality gives $F \to 0$ at the past endpoint. For $u = 0$, $J(a) = 2a^{3/2}/3$ and the pure-dust bound is recovered.

The conserved dust–radiation mixture has pressure ratio $w_B(a) = \Omega_{r0}/[3(\Omega_{m0} a + \Omega_{r0})]$. Differentiating $E = E_B Y$ and subtracting the radiation pressure gives

$$\begin{aligned} \frac{P_X}{\varepsilon_{\rm tot}} &= F w_B - \frac{s}{E}, \\ w_{X0} = -1 \quad &\Longleftrightarrow \quad s = (1 - M)(1 + u^2/3). \end{aligned} \tag{A5}$$

For $\Omega_{m0} = 0.30$ and $\Omega_{r0} = 9.2 \times 10^{-5}$, matching $w_{X0} = -1$ requires $s = 0.699980$. The crossing $Y = \sqrt{M}$ occurs at $a_{\rm on} = 0.500378$, or $z_{\rm on} = 0.998487$. The shift from the dust-only benchmark is 6.18×10^{-5} in scale factor.

Combining the same pressure calibration with the all-past bound gives

$$\sqrt{M} \leq \frac{2u^2(1 - u)}{(1 + 2u)(3 + u^2)}. \tag{A6}$$

The right side vanishes for either pure constituent. At $u = 1/2$, it equals $1/26$. Thus $\Omega_{m0} = 0.00075$ and $\Omega_{r0} = 0.00025$ satisfy the inequality and allow $w_{X0} = -1$ with a nonnegative fraction throughout the past.

A.3 A variable rate that stays admissible

With dust as the other source, keep the critical normalization and set $\Gamma_{\rm eff} = 3HF$. Then $\dot{F} = 3HF(1 - F)$, whose integral satisfies $d \ln[F/(1 - F)]/d \ln a = 3$. Using Eq. (16) with $0 < F_0 < 1$ gives

$$F(a) = \frac{F_0 a^3}{1 - F_0 + F_0 a^3}, \qquad E^2(a) = (1 - F_0) a^{-3} + F_0. \tag{A7}$$

The product $FE^2 = F_0$ is constant. Thus $P_X = -\varepsilon_X = -F_0 \varepsilon_{\rm crit,0}$, and $0 < F < 1$ for every $a > 0$. These functions reproduce the $\epsilon = 3$ case of Eqs. (26)–(27) of Durán & Parisi (2012), with $\widetilde{r}_0 = (1 - F_0)/F_0$. An independent origin for this rate would be needed to explain the constant density.

At common H_0, $0 < \Omega_{m0} < 1$, and $w_{X0} = -1$, both rates give $F_0 = 1 - \Omega_{m0}$ and $q_0 = (3\Omega_{m0} - 2)/2$. The constant rate also requires $s = F_0$. The first local difference occurs in the third time derivative of the scale factor. The jerk $j = \dddot{a}/(aH^3) = q(1 + 2q) - dq/d \ln a$ gives

$$j_0^{\text{constant rate}} = 1 - \frac{9}{4} \Omega_{m0} (1 - \Omega_{m0}), \qquad j_0^{\text{variable rate}} = 1. \tag{A8}$$

At $\Omega_{m0} = 0.30$ the predicted present jerks are 0.5275 and 1. A measurement of that derivative could distinguish the two specified rate laws even over a redshift interval where both residual densities are positive.

APPENDIX B: CAPACITY ON A SPECIFIED EXPANSION HISTORY

A constant density on the reference background can exhaust a reserve for the apparent horizon and remain admissible for the event horizon. Yet these horizons approach the same proper radius. The distinction turns on what has been held fixed across the two prescriptions. We first express the capacity as a length, and then keep the event prescription identical in two calibrations of the other horizons.

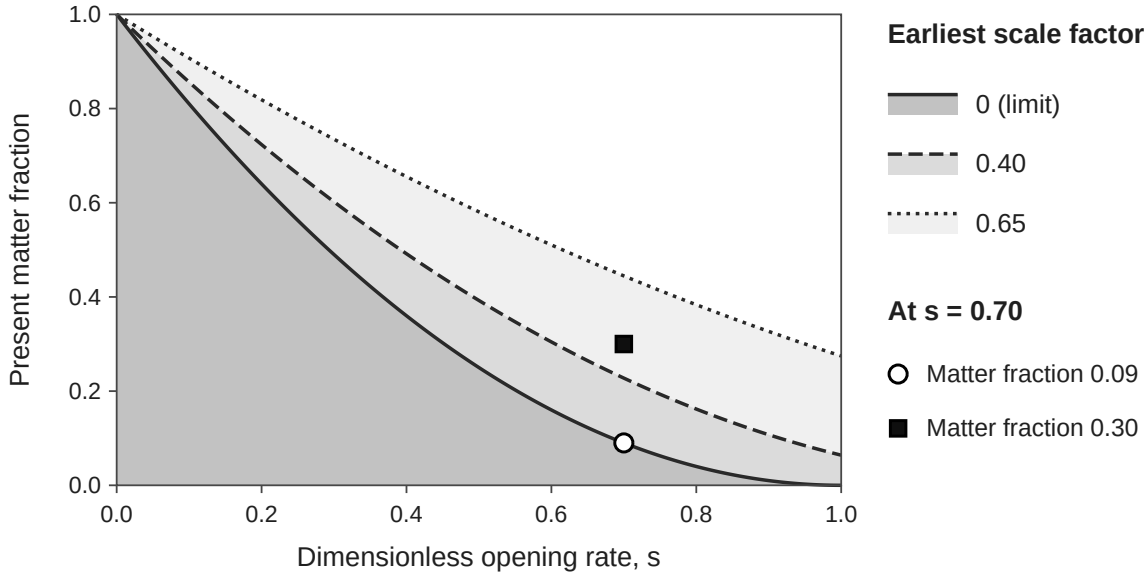


FIGURE A1 Maximum assigned dust fraction at each rate for three lookback intervals ending today. Admissible points lie on or below their respective curve. The circle and square have the same expansion history. The circle lies on the boundary for positivity throughout the past. The square survives to $a = 0.65$ but fails before $a = 0.40$. The endpoints of the rate range represent limits of $0 < s < 1$.

Let $Q_{\mathrm{tot}} > 0$ be a fixed reserve and $F_X \in [0, 1]$ its accessible fraction for horizon X. A model with measure $C_X R_X^D$, $D > 0$ and constant $C_X > 0$, assigns energy density

$$\varepsilon_X = \frac{Q_{\mathrm{tot}} F_X}{C_X R_X^D}, \qquad [C_X] = \frac{[Q_{\mathrm{tot}}]}{[\varepsilon_X]\,[\mathrm{length}]^D}. \tag{B9}$$

When $D = 2$ and Q_{tot} is an energy, C_X has dimensions of length. In the inverse-square prescription used above $B = Q_{\mathrm{tot}}/C_X$ for the chosen horizon. Radicella & Pavón (2010) reconstructed the coefficient for a fixed vacuum density at the particle and Hubble radii and tested how slowly it varies. For the particle radius their coefficient is proportional to R_p^2. Here a finite upper amplitude sets a maximum admissible radius even when the rate of variation is unrestricted. A capacity test requires a physical upper bound on that amplitude.

B.1 Reference expansion

For the calibrated comparisons fix a radiation–matter–vacuum background with $E = H/H_0$, $H_0 = H(t_0)$, and

$$E^2(a) = \Omega_{r0} a^{-4} + \Omega_{m0} a^{-3} + \Omega_\Lambda,$$
$$(\Omega_{r0}, \Omega_{m0}, \Omega_\Lambda) = (0.000092, 0.30, 0.699908). \tag{B10}$$

This equation specifies the complete expansion on which the three candidate densities are evaluated. Each uses the same radiation-dominated early history and asymptotically exponential future. All three horizons are finite at every positive finite a. Their present radii in units of c/H_0 are 3.24191, 1, and 1.14072 in particle, apparent and event order. Appendix E gives the corresponding growth rates.

B.2 The radius that exhausts a reserve

For a constant positive target ε_* on an interval I containing $a_0 = 1$, Eq. (B9) fixes

$$F_X(a) = F_{X0} \left(\frac{R_X(a)}{R_{X0}} \right)^D, \qquad F_{X0} = \frac{\varepsilon_* C_X R_{X0}^D}{Q_{\mathrm{tot}}}. \tag{B11}$$

Here R_X is positive and finite at each epoch of I. Setting $M_X(I) = \sup_{a \in I} R_X(a)$, the stipulated positive fraction at $a = 1$ is admissible throughout I precisely when

$$F_{X0} \le \left[\frac{R_{X0}}{M_X(I)} \right]^D. \tag{B12}$$

This follows by taking the supremum in Eq. (B11). Equality includes a radius approached only at an endpoint. An infinite supremum excludes every positive reference fraction, even if each instantaneous radius is finite.

Suppose $C_X = C$, $Q_{\rm tot}$ and ε_* are common. The same test takes the form

$$R_{\rm cap} = \left(\frac{Q_{\rm tot}}{\varepsilon_* C}\right)^{1/D}, \qquad F_X(a) = \left(\frac{R_X(a)}{R_{\rm cap}}\right)^{D}, \qquad M_X(I) \le R_{\rm cap}. \tag{B13}$$

A single physical ceiling then applies to all three radii. In comparison, fixing three equal present fractions fixes three equal values of $C_X R_{X0}^D/Q_{\rm tot}$, which generally entails different ceilings. An independent restriction on the rate of access could further reduce the admissible domain. For a constant target the required rate is $\dot F_X/F_X = D\dot R_X/R_X$.

For a positive, evolving target $\varepsilon_{\rm tar}$ the exact test becomes

$$F_{X0}\sup_{a\in I}\left[\frac{\varepsilon_{\rm tar}(a)}{\varepsilon_{\rm tar}(1)}\left(\frac{R_X(a)}{R_{X0}}\right)^{D}\right] \le 1. \tag{B14}$$

Both factors are evaluated at the same epoch. A decreasing target can compensate for an unbounded radius. Maximizing each factor separately can exclude admissible histories when the peaks occur at different epochs.

B.3 The same event horizon under two calibrations

Which radius reaches a physical ceiling first? For the reference history of Eq. (B10), a ceiling $R_{\rm cap} = 1.16c/H_0$ is reached by the event radius at $a_e = 1.178585$ and by the apparent radius at $a_A = 1.907152$. Both eventually exceed it. A comparison at equal present fractions can give a different verdict even on this identical expansion.

Take $D = 2$, a constant target, and write $\widehat R = H_0 R/c$. Since H decreases to $H_0\sqrt{\Omega_\Lambda}$, the apparent and event radii grow to $\widehat R_\infty = 1/\sqrt{\Omega_\Lambda} = 1.195307$ to the accuracy shown. The particle radius grows without bound since its comoving radius is already positive and nondecreasing. At the reference epoch $\widehat R_{A0} = 1$ and

$$\widehat R_{e0} = \int_0^1 \frac{du}{\sqrt{\Omega_\Lambda + \Omega_{m0}u^3 + \Omega_{r0}u^4}} \simeq 1.140725. \tag{B15}$$

Equation (B12) gives the full-future upper bounds on present utilization as 0, 0.699908 and 0.910757 for the particle, apparent and event prescriptions. The apparent and event bounds differ because their present radii differ. For example, $F_{A0} = \Omega_\Lambda$ gives exactly $F_A = \Omega_\Lambda/E(a)^2$, the instantaneous vacuum fraction of this background. If the reserve represents that vacuum term it is counted only once in the density budget.

Calibration at equal present fractions.

Set each present fraction to 0.80 in Fig. B2 (a). The apparent radius can grow only to $1/\sqrt{0.80} = 1.11803$ in Hubble-length units before the reserve is exhausted. Its required fraction tends to 1.1430. The larger present event radius instead implies a ceiling of $1.140725/\sqrt{0.80} = 1.27537$ and a limiting fraction of 0.87839. The particle prescription crosses its finite ceiling as well.

Calibration at a common radius.

In Fig. B2 (b) keep the event prescription unchanged at every epoch and use its ceiling 1.27537 for all three horizons. At the same constant target this gives a present apparent fraction of $0.80/\widehat R_{e0}^2 = 0.614792$ to the accuracy shown. The apparent and event fractions now both tend to 0.87839. The required particle fraction is 6.4615 already today. The change in the apparent calibration reverses its long-term verdict while the target density, expansion history and limiting radius remain fixed.

A finite interval.

The intermediate ceiling $1.16c/H_0$ lies above both present radii and below their common limit. Between the two crossing epochs the apparent prescription remains admissible and the event prescription has already exhausted the reserve (Table B1). The endpoint radii suffice for this test because the two histories are monotone. Exact equality corresponds to full utilization, with violation immediately afterward.

TABLE B1 Capacity over $1 \le a \le a_f$ for a common radius ceiling $1.16c/H_0$. Each verdict applies to the entire closed interval.

a_f	$\widehat R_A(a_f)$	$\widehat R_e(a_f)$	Apparent	Event
1.00	1.00000	1.14072	admissible	admissible
1.15	1.05573	1.15757	admissible	admissible
1.20	1.06992	1.16169	admissible	excluded
1.50	1.12593	1.17729	admissible	excluded
2.00	1.16451	1.18748	excluded	excluded

An independent interval of allowed physical ceilings excludes a model only if the required maximum radius exceeds every allowed ceiling. The chosen future expansion enters this comparison even when testing a fairly short interval. For an accelerating future power law $a \propto t^\nu$, $\nu > 1$, both $R_A = ct/\nu$ and $R_e = ct/(\nu-1)$ diverge at late times. On that continuation neither radius can sustain a positive constant target indefinitely with a bounded reserve.

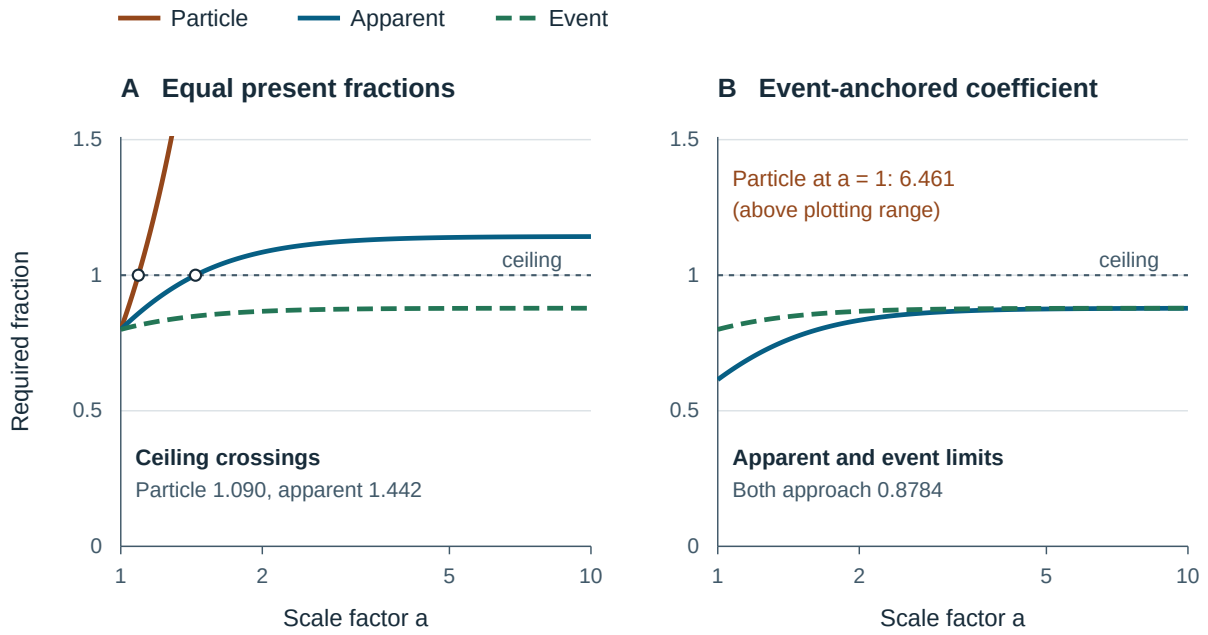


FIGURE B2 Required reserve fractions for a constant density with $D = 2$. The event prescription is identical in both panels. Panel (a) fixes all present fractions at 0.80. Panel (b) fixes one radius ceiling at the event-calibrated value. The apparent fraction starts at 0.614792 in (b) and approaches the same limit as the event fraction. The particle fraction is 6.4615 already at $a = 1$. Values above unity exceed the reserve.

APPENDIX C: CAN THE HORIZONS REQUIRE THE SAME ACCESSIBILITY HISTORY?

The absolute ceiling in Eq. (B13) depends on the conversion from a radius to an accessible fraction. The relative evolution of two candidate fractions admits a comparison independent of that conversion. In particular, a difference in normalization can make the particle and event prescriptions agree at one epoch only. This follows directly from the opposite null-boundary terms in their radius equations.

C.1 Removing the unknown constants

Consider a connected interval I of an expanding flat FLRW spacetime on which the candidate radii are finite and positive. Prescribe the same positive density history $\varepsilon_*(t)$ and exponent $D > 0$ for both. Each horizon may have its own constant $k_X = C_X/Q_{\mathrm{tot},X} > 0$, so the fraction required by Eq. (B9) is $F_X = k_X \varepsilon_* R_X^D$. Choose $t_0 \in I$, let $U_X = F_X(t)/F_X(t_0)$, and form

$$\mathcal{D}_{XY}(t) = \frac{U_X(t)}{U_Y(t)} = \left[\frac{R_X(t)/R_Y(t)}{R_X(t_0)/R_Y(t_0)}\right]^D . \tag{C16}$$

The normalization within each prescription removes k_X. Comparing prescriptions then removes the shared density history, including any time variation. The two normalized histories agree throughout I exactly when R_X/R_Y is constant. Equality at two isolated epochs generally allows a varying ratio between them. The identity still describes formal requirements exceeding unit capacity. It carries no information about their absolute magnitudes.

For Eq. (B10) set $D = 2$ and choose the present as the reference epoch. The predicted double ratios are

Scale factor a	$\mathcal{D}_{Ae}$	$\mathcal{D}_{eA}$	$\mathcal{D}_{pe}$
1	1.0000	1.0000	1.0000
1.5	1.1902	0.8402	2.6016
2	1.2514	0.7991	5.0419
$a \to \infty$	1.3013	0.7685	∞

At twice the present scale factor the growth factor required at the apparent radius is 1.2514 times that required at the event radius. Their common limiting proper radius gives $\mathcal{D}_{Ae} \to (R_{e0}/R_{A0})^2$. In the same comparison the unbounded particle radius drives $\mathcal{D}_{pe}$ to infinity.

C.2 A strict ordering of the causal-horizon predictions

The relative particle-to-event trend has a definite sign in every background satisfying the hypotheses. By Eqs. (31) and (C16),

$$\frac{d}{dt}\ln\left(\frac{F_p}{F_e}\right) = \frac{d}{dt}\ln \mathcal{D}_{pe} = Dc\left(\frac{1}{R_p}+\frac{1}{R_e}\right) > 0. \quad \text{(C17)}$$

The terms proportional to H cancel. With expansion factored out, a comoving null interval is added to the accumulated particle distance and removed from the remaining event distance. The two normalized predictions therefore separate strictly after any chosen reference epoch, even when each individual fraction is nonmonotone. With exact input, a second epoch suffices to distinguish their relative evolution.

C.3 The apparent radius and constant shape ratios

Set $x = R_e/R_A = HR_e/c$. Using $\dot{R}_e = HR_e - c$ yields (Margalef-Bentabol et al., 2013)

$$\frac{dx}{d\ln a} = -1 - qx, \qquad \frac{d\ln \mathcal{D}_{eA}}{d\ln a} = -D\left(q+\frac{1}{x}\right). \quad \text{(C18)}$$

A constant $x > 0$ on an open interval requires a constant negative $q = -1/x$. For an accelerating power law $a \propto t^\nu$, $\nu > 1$, continued to the infinite future, $x = \nu/(\nu-1)$. For exponential expansion with its exponential future, $x = 1$. Similarly $y = R_p/R_A$ obeys $dy/d\ln a = 1 - qy$, so constant $y > 0$ requires constant positive $q = 1/y$, as realized in a universe always filled with pressureless matter. All three finite radii cannot remain proportional on an open interval.

A constant q measured over a finite interval leaves an undetermined boundary term in x. Consider exponential expansion with constant $H_* > 0$ up to time T, followed by the continuously differentiable continuation

$$a(t) = a(T)[1 + H_*(t-T)/2]^2, \qquad t \geq T. \quad \text{(C19)}$$

Integration of the future tail gives $R_e(T) = 2c/H_*$. Splitting the defining integral at T then gives $x(t) = 1 + \exp[H_*(t-T)]$ within the preceding exponential segment. Although $q = -1$ there, the relative history varies.

To use these relations with a single measured fraction history one must independently constrain the relative evolution of the target density. Otherwise each prescription can fit $F_{\rm obs}(t)$ by assigning it a different target, $\varepsilon_{*,X} = F_{\rm obs}/(k_X R_X^D)$. With a common target fixed, the double ratio compares predictions even when the absolute reserve is unknown. Time-dependent conversion factors or unequal exponents introduce additional time dependence and require their own calibration.

APPENDIX D: PRESSURE AND DEGENERACY AT FIXED EXPANSION

For a horizon of finite, positive proper radius R_X, let

$$S_X = C_X R_X^D, \qquad \varepsilon_X = \frac{Q_X}{S_X}, \qquad C_X > 0, \quad D > 0. \quad \text{(D20)}$$

Here C_X and D are constant. If the numerator Q_X is an energy, S_X has units of volume and the area prescription $D = 2$ requires C_X to have units of length. The inverse-square dependence also occurs in holographic dark-energy models (Hsu, 2004; Li, 2004).

At epochs with differentiable $Q_X > 0$, let $\gamma_X = d\ln R_X/d\ln a$. Logarithmic differentiation yields

$$\eta_X = \frac{d\ln Q_X}{d\ln a}, \qquad n_X = -\frac{d\ln \varepsilon_X}{d\ln a} = D\gamma_X - \eta_X. \quad \text{(D21)}$$

A prescribed positive density history $\varepsilon_\star$ fixes the numerator at each epoch,

$$Q_X = C_X R_X^D \varepsilon_\star. \quad \text{(D22)}$$

In particular, $\eta_X = D\gamma_X$ maintains constant density even for a growing radius. The freedom to reconstruct an amplitude is familiar from time-dependent holographic coefficients (Durán & Parisi, 2012; Radicella & Pavón, 2010). A capacity or rate constraint on Q_X can test such a reconstruction.

D.1 Separate conservation and pressure

For separate conservation, with P_X and ε_X in the same units, the inferred pressure obeys

$$\begin{aligned} &\dot{\varepsilon}_X + 3H(\varepsilon_X + P_X) = 0, \\ &w_X = \frac{P_X}{\varepsilon_X} = -1 + \frac{D\gamma_X - \eta_X}{3}. \end{aligned} \quad \text{(D23)}$$

With transfer J_X into the component on the right of the continuity equation, the dilution measures the combination $n_X = 3(1+w_X) - J_X/(H\varepsilon_X)$. An independent transfer law is then needed to extract P_X.

At constant numerator and $D = 2$, the radius slopes of Eq. (31) give

$$\begin{aligned} w_p &= -\frac{1}{3} + \frac{2c}{3HR_p}, \\ w_A &= \frac{2q-1}{3} = w_{\rm tot}, \\ w_e &= -\frac{1}{3} - \frac{2c}{3HR_e}. \end{aligned} \quad \text{(D24)}$$

The equality to $w_{\rm tot} = P_{\rm tot}/\varepsilon_{\rm tot}$ uses the flat Einstein equations and counts any vacuum energy among the sources. The particle and event prescriptions fall on opposite sides of $w = -1/3$ (Li, 2004). The event component has $w_e < -1$ precisely where $HR_e < c$ and the proper event radius shrinks. These component pressures enter the acceleration equation through the sum of $\varepsilon_i + 3P_i$ over all sources. Figures E4 and E5 give the histories on the reference expansion.

D.2 The apparent radius tracks the total density

Write $B = Q_A/C_A$ and hold B and G constant. Substituting $R_A = c/H$ in the Friedmann constraint gives

$$\varepsilon_A = \frac{BH^2}{c^2}, \qquad \varepsilon_{\rm tot} = \frac{3c^2H^2}{8\pi G}, \qquad f = \frac{\varepsilon_A}{\varepsilon_{\rm tot}} = \frac{8\pi GB}{3c^4}. \tag{D25}$$

The apparent component therefore carries a constant fraction of the total. If $0 < f < 1$ and the remaining sources are conserved dust and radiation,

$$\varepsilon_{\rm tot}(a) = \frac{\varepsilon_{m0}a^{-3} + \varepsilon_{r0}a^{-4}}{1-f}. \tag{D26}$$

For dust alone $H \propto a^{-3/2}$ and $q = 1/2$. With positive radiation the total pressure remains nonnegative. A constant f changes the expansion normalization while preserving deceleration in either case (Hsu, 2004; Li, 2004). At $f = 1$ with the other sources absent, the Friedmann constraint fixes B and leaves the expansion undetermined. For the event prescription one must also impose the future null-boundary condition when solving for an expansion (Li, 2004).

D.3 Two matter assignments with identical horizons

Retain the same radiation and vacuum normalization as in Eq. (B10). One model assigns $0.30a^{-3}$ to dust and Ω_Λ to vacuum, in present critical-density units. A second assigns $0.20a^{-3}$ to dust and the following density and pressure to a component U, in the same units.

$$\varepsilon_U = \Omega_\Lambda + 0.10a^{-3}, \qquad P_U = -\Omega_\Lambda, \qquad w_U = -\frac{\Omega_\Lambda}{\Omega_\Lambda + 0.10a^{-3}}. \tag{D27}$$

The second assignment obeys separate conservation since $d\varepsilon_U/d\ln a = -0.30a^{-3} = -3(\varepsilon_U + P_U)$. The component U evolves from dust-like to vacuum-like pressure relative to its density. Nevertheless, at every epoch the two models have identical total density and pressure, and hence identical expansion and corresponding horizon radii for the same past and future boundaries. This is an explicit background degeneracy (Kunz, 2009). Perturbations would distinguish these assignments only if their specified dynamics gave different predictions.

APPENDIX E: HORIZON GROWTH AND EFFECTIVE-FLUID DIAGNOSTICS

On the reference expansion of Eq. (B10), the particle radius retains the accumulated conformal past. Its comoving value tends to a positive constant, giving $R_p \propto a$ asymptotically and $\gamma_p > 1$ at finite epochs. Both R_A and R_e approach c/H_∞ and their slopes approach zero. The event radius during matter domination already depends on the later vacuum-dominated expansion.

Figure E4 compares Eq. (D24) with the independent background pressure $w_{\rm tot} = (\Omega_{r0}a^{-4}/3 - \Omega_\Lambda)/E^2$. For an entirely dust-filled universe $R_p = 2R_A$. Both radii grow as $a^{3/2}$, giving $w_p = w_A = 0$. On the reference background the particle radius retains the radiation era in its past integral, so the two pressure curves can differ during matter domination.

A fixed numerator and an area law give $n = 2$ only when the proper radius grows proportionally to a at that epoch. Pure radiation and pure dust instead give $n_p = n_A = 4$ and 3, respectively. On the late vacuum-dominated reference expansion the particle curve tends to two from above. A positive constant target at the particle radius would then require $Q_p \propto a^2$ asymptotically. For the apparent and event radii a constant target requires only a finite limiting numerator.

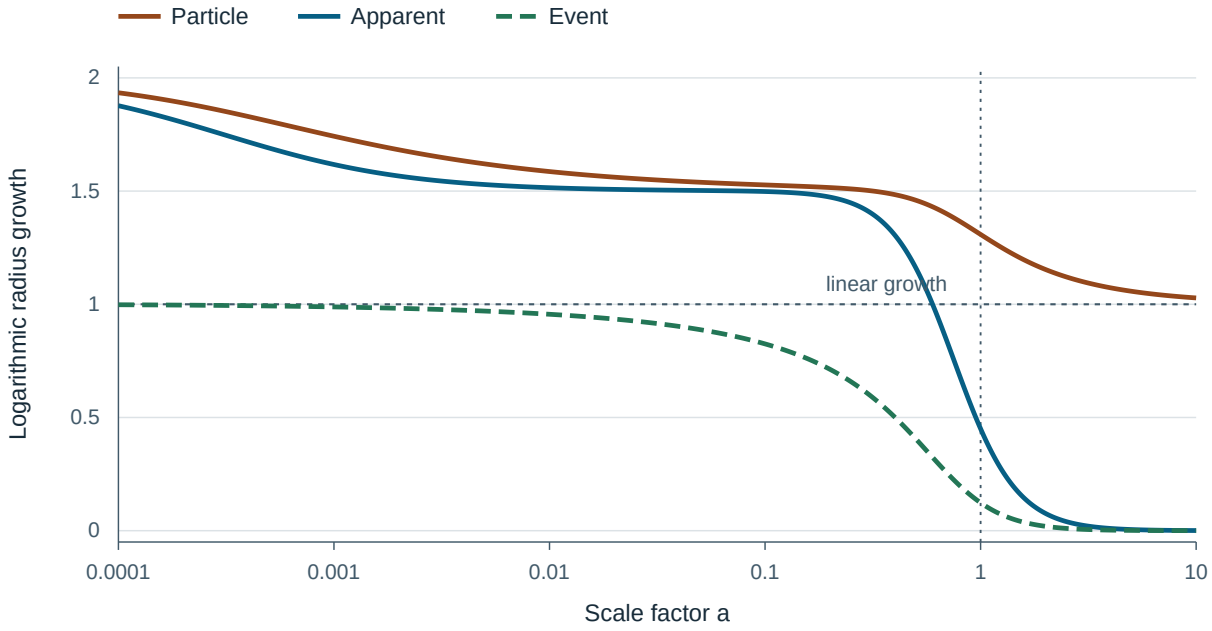


FIGURE E3 Logarithmic growth $\gamma_X = d \ln R_X / d \ln a$ for the three proper radii on the radiation–matter–vacuum background. The horizontal line marks $R_X \propto a$ locally. The vertical line marks today.

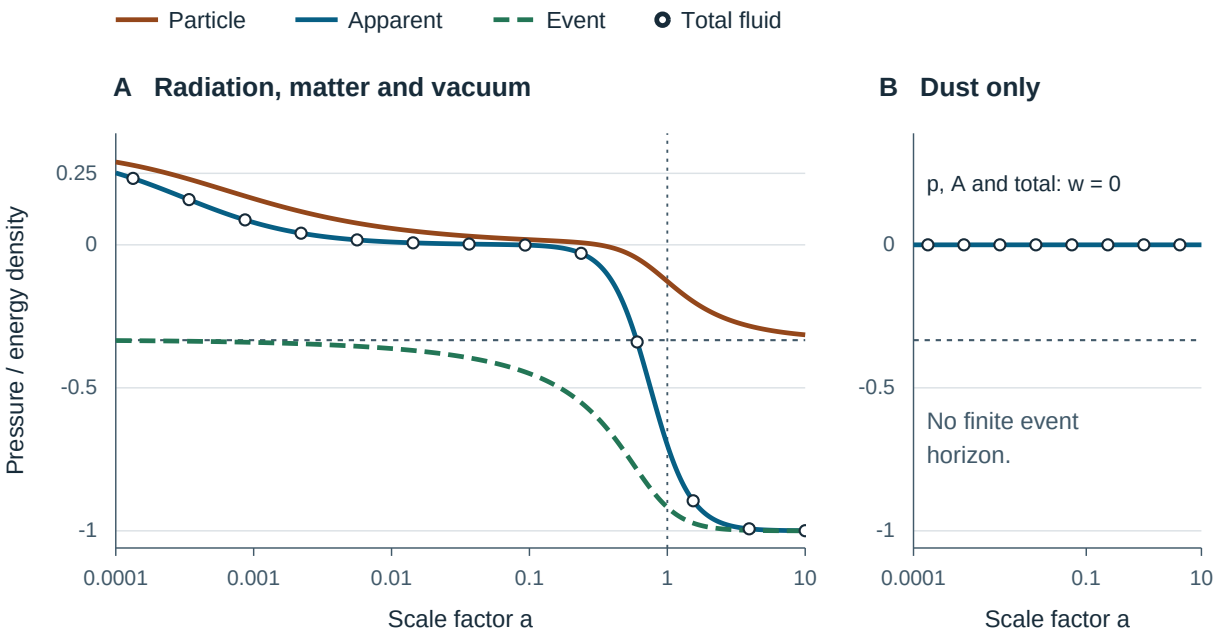


FIGURE E4 Pressure-to-density ratios for $D = 2$, constant Q_X and separate conservation. In panel A the apparent-horizon curve overlaps the directly calculated total pressure ratio on Eq. (B10). In panel B the particle and apparent radii of a pure-dust universe give the same pressure ratio. There is no finite event horizon in that model.

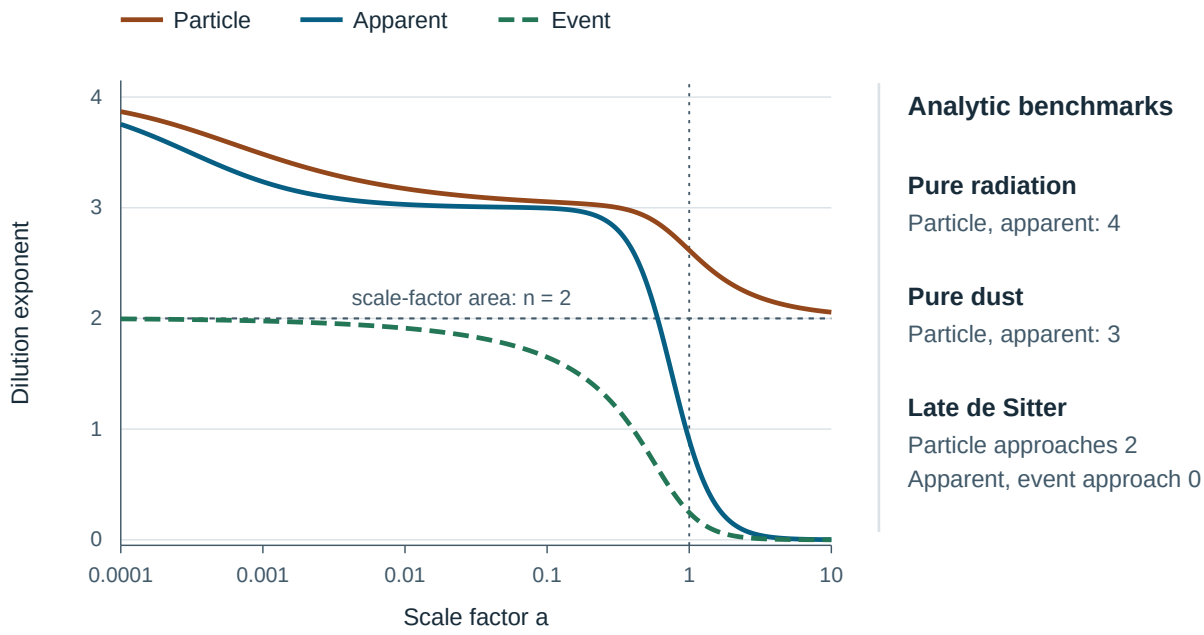


FIGURE E5 Dilution exponent $n_X = 2\gamma_X$ at fixed numerator, evaluated on the reference expansion. The horizontal line marks the inverse-square dilution of a radius growing locally in proportion to a.

APPENDIX F: NUMERICAL METHODS AND INDEPENDENT CHECKS

F.1 Particle-horizon trajectory

Figure 1 evolves a and $x = \chi_p/(cT)$ from the exact dust initial data at $t = T$. The figure program integrates Eq. (2) with a fourth-order Runge–Kutta method in $\ln(t/T)$ and evaluates the acceleration from the differentiated constraint. Bisection on the two changes of sign gives the shaded interval. Halving the integration step changes the dimensionless crossing times by less than 10^{-9}. An independent integration in t/T gives $T^2\ddot{a} = 0.92743$ at the midpoint, in agreement with a centered difference of the computed expansion speed. At the first acceleration crossing the initial state also determines the upper duration through Eq. (5). For the continuous-pressure example, integrating the dimensionless particle radius in $\sqrt{a}$ directly from the big bang gives the exit $a = 1.42609756$. A separate calculation starts on the analytic early branch, integrates in $\ln a$, and checks the same exit and both joins. The late-time limit follows analytically from the bound in Section 2.

The supplementary equation-based verification also integrates these trajectories with adaptive DOP853, using relative tolerance 2.5×10^{-13}. It repeats the rapid-ramp calculation with a, instead of t/T, as the independent variable, and compares the continuous-pressure calculation in $\sqrt{a}$ with an integration in $\ln a$. The acceleration crossings agree within 2×10^{-11} in their respective dimensionless variables. The supplied Runge–Kutta, duration, radiation and rate-law verification programs were also rerun; the supplement records their outputs and step-refinement comparisons.

F.2 Horizon integrals and endpoint conditions

Set $r_X = H_0 R_X/c$, $E = H/H_0$ and $a(t_0) = 1$. With $\Omega_r, \Omega_m, \Omega_\Lambda$ the present density fractions of Eq. (B10), the dimensionless comoving radii are

$$I_p(a) = \frac{r_p(a)}{a} = \int_0^a \frac{dx}{\sqrt{\Omega_r + \Omega_m x + \Omega_\Lambda x^4}}, \tag{F28}$$

$$I_e(a) = \frac{r_e(a)}{a} = \int_0^{1/a} \frac{dy}{\sqrt{\Omega_\Lambda + \Omega_m y^3 + \Omega_r y^4}}. \tag{F29}$$

The inverse scale factor y brings the infinite future to $y = 0$. Using the plotted endpoints as the limits of the past or future integral would instead force a null radius at a finite epoch in the benchmark.

The curves sample 801 logarithmically spaced values of a from 10^{-4} through 10, including unity. The figure program uses 48-point Gauss–Legendre quadrature, splitting the particle integral at the powers of ten between 10^{-5} and unity interior to its domain. It computes $T = I_p(1) + I_e(1)$. For $a < 1$ it evaluates I_p and forms $I_e = T - I_p$. For $a \geq 1$ it evaluates I_e and forms $I_p = T - I_e$. Constancy of this sum is built into the procedure.

A separate implementation evaluates each horizon integral directly using composite Simpson quadrature with 4096 panels. In the particle integral it uses $x = au^4$ to resolve the early radiation term. For the event radius the resolving substitution $y = u^4/a$ gives

$$r_e(a) = \int_0^1 \frac{4u^3\,du}{\sqrt{\Omega_\Lambda + \Omega_m(u^4/a)^3 + \Omega_r(u^4/a)^4}}. \tag{F30}$$

The figure program also compares its Gauss–Legendre values against a 16384-panel Simpson evaluation at six epochs and at the calibration crossings. In this additional check, the future integral for $a < 1$ is split at unit scale factor. All threshold roots are bracketed by the corresponding monotone radius histories and located by bisection.

The supplementary verification evaluates both horizon integrals directly by adaptive quadrature, without imposing constancy of $I_p + I_e$, and compares them with the fourth-power Simpson rules over the full 801-point grid. The largest relative differences with 4096 panels are 1.17×10^{-13} for the particle radius and 1.30×10^{-12} for the event radius. With 8192 panels they are below 7.5×10^{-15} and 8.2×10^{-14}, respectively. These are numerical comparisons on the stated grid, not rigorous error bounds over a continuous interval. The reported radii, calibrations and trajectory values are unchanged at their quoted precision.

F.3 Reference values and calibrations

The exact logarithmic slopes in particle, apparent and event order are

$$1 + \frac{1}{Er_p}, \qquad \frac{2\Omega_r a^{-4} + (3/2)\Omega_m a^{-3}}{E^2}, \qquad 1 - \frac{1}{Er_e}. \tag{F31}$$

Evaluated at $a = 1$, the quadratures and derivatives give

Quantity	Particle	Apparent	Event
$H_0 R_X/c$	3.24191240	1.00000000	1.14072451
$d\ln R_X/d\ln a$	1.30845991	0.45018400	0.12336415
F_X, common coefficient in Fig. B2	6.461465	0.614792	0.800000

Near $a = 10^{-4}$, neglecting the vacuum term gives

$$r_p(a) \simeq \frac{2a^2}{\sqrt{\Omega_r + \Omega_m a} + \sqrt{\Omega_r}}.$$

The particle slope is 1.93419 at the first sample. The finite matter fraction accounts for its departure from the pure-radiation value of two. The independently calculated total pressure ratio in Fig. E4 agrees with the apparent-horizon pressure over the full grid.

Figure B2 compares the prescriptions

$$F_X = 0.80 \left[\frac{r_X(a)}{r_X(1)}\right]^2, \qquad F_X = 0.80 \left[\frac{r_X(a)}{r_e(1)}\right]^2 .$$

The event curves coincide at all sampled epochs. With the common coefficient the apparent and event fractions both approach 0.8783902 as their radii approach $1/\sqrt{\Omega_\Lambda}$. Imposing an independent ceiling of $1.16\,c/H_0$ gives $F_X = [r_X(a)/1.16]^2$ and the forward event and apparent crossings $a = 1.178585$ and 1.907152, respectively. Values $F_X > 1$ mark the portion of the algebraically continued curve outside the physical domain.

F.4 Dust subtraction and rate-law checks

For the illustrative thirty per cent assignment in Table 1 , the numerical check takes $\Omega_{m0} = 0.30$, $s = \Gamma/(3H_0) = 0.70$ and evaluates $E = s + (1 - s)a^{-3/2}$. Subtraction of $\Omega_{m0}a^{-3}$ from E^2 gives the residual density in present critical-density units. Dividing the residual by E^2 reproduces Eq. (24). Inserting the analytic past boundary gives zero within roundoff. The table quotes w_X only on the positive-density branch.

For the dust–radiation mixture in Appendix A.2, direct quadrature of J in Eq. (A3) and bisection verify the crossings calculated from the analytic integral. The verification also checks a dilute mixed solution admissible over the entire past. For the rate comparison, centered first and second differences of E^2 at $a = 1$, with scale-factor step 10^{-7} and 60-digit arithmetic, reproduce the two jerk values in Eq. (A8). A further difference calculation checks the variable-rate fraction's differential equation at five distinct scale factors.

REFERENCES

Abdollahi Zadeh, M., Sheykhi, A., Moradpour, H., & Bamba, K. 2018, *European Physical Journal C*, *78*, 940. doi: 10.1140/epjc/s10052-018-6427-3

Avelino, A., & Nucamendi, U. 2009, *Journal of Cosmology and Astroparticle Physics*, *2009*(04), 006. doi: 10.1088/1475-7516/2009/04/006

Cai, R.-G., & Kim, S. P. 2005, *Journal of High Energy Physics*, *2005*(02), 050. doi: 10.1088/1126-6708/2005/02/050

Carvalho, F. C., Alcaniz, J. S., Lima, J. A. S., & Silva, R. 2006, *Physical Review Letters*, *97*, 081301. doi: 10.1103/PhysRevLett.97.081301

Cruz, M., & Lepe, S. 2020, *Nuclear Physics B*, *956*, 115017. doi: 10.1016/j.nuclphysb.2020.115017

Davis, T. M., & Lineweaver, C. H. 2004, *Publications of the Astronomical Society of Australia*, *21*, 97–109. doi: 10.1071/AS03040

Durán, I., & Parisi, L. 2012, *Physical Review D*, *85*, 123538. doi: 10.1103/PhysRevD.85.123538

Fazlollahi, H. R. 2023, *Chinese Physics C*, *47*, 035101. doi: 10.1088/1674-1137/aca468

Harrison, E. 1991, *The Astrophysical Journal*, *383*, 60–65. doi: 10.1086/170763

Hsu, S. D. H. 2004, *Physics Letters B*, *594*, 13–16. doi: 10.1016/j.physletb.2004.05.020

Kunz, M. 2009, *Physical Review D*, *80*, 123001. doi: 10.1103/PhysRevD.80.123001

L'Huillier, B., Shafieloo, A., & Kim, H. 2018, *Monthly Notices of the Royal Astronomical Society*, *476*, 3263–3268. doi: 10.1093/mnras/sty398

Li, M. 2004, *Physics Letters B*, *603*, 1–5. doi: 10.1016/j.physletb.2004.10.014

Lima, J. A. S., Silva, F. E., & Santos, R. C. 2008, *Classical and Quantum Gravity*, *25*, 205006. doi: 10.1088/0264-9381/25/20/205006

Margalef-Bentabol, B., Margalef-Bentabol, J., & Cepa, J. 2013, *Journal of Cosmology and Astroparticle Physics*, *2013*(02), 015. doi: 10.1088/1475-7516/2013/02/015

Radicella, N., & Pavón, D. 2010, *Journal of Cosmology and Astroparticle Physics*, *2010*(10), 005. doi: 10.1088/1475-7516/2010/10/005

Re Fiorentin, M., & Re Fiorentin, S. 2023, *American Journal of Physics*, *91*, 644–652. doi: 10.1119/5.0127840

Rindler, W. 1956, *Monthly Notices of the Royal Astronomical Society*, *116*, 662–677. doi: 10.1093/mnras/116.6.662